Available online at www.sciencedirect.com
ScienceDirect
ELSEVIER
Earth and Planetary Science Letters xx (2007) xxx–xxx
EPSL
www.elsevier.com/locate/epsl

Combining [^{3}He] cosmogenic dating with U–Th/He eruption ages using olivine in basalt

Sarah M. Aciego [a,b,*], Donald J. DePaolo [a,b], B.M. Kennedy [a], Michael P. Lamb [b], Kenneth W.W. Sims [c], William E. Dietrich [b]

[a] *Earth Sciences Division, E.O. Lawrence Berkeley National Laboratory, Berkeley, CA 94720, United States*
[b] *Department of Earth and Planetary Science, University of California, Berkeley, CA 94720-4767, United States*
[c] *Department of Geology and Geophysics, Woods Hole Oceanographic Institution, Woods Hole, MA 02543, United States*

Received 13 July 2006; received in revised form 21 November 2006; accepted 22 November 2006

Editor: R.W. Carlson

Abstract

This paper presents new U–Th/He crystallization and ^{3}He exposure ages on olivine for a suite of basalt samples from the Snake River Plain, Idaho. The results provide the first demonstration that U–Th/He geochronology can be successfully applied to Late Quaternary basalts using measurements of olivine phenocrysts as opposed to U-rich minerals. The approach employs abrasion to remove the outer rinds of olivine crystals to avoid problems with ^{4}He implantation from the groundmass, and a specially designed extraction system that allows U, Th and He concentrations and isotopic compositions to be measured on the same olivine grains. We demonstrate the viability of the U–Th/He technique on basalts with ages of 373 ka and 3400 ka previously dated by Ar–Ar, and show that concurrent measurements of U–Th–^{4}He ages and ^{3}He cosmogenic exposure ages improve the accuracy of both methods. The combined U–Th–^{4}He–^{3}He technique is applied to a series of boulders and flows from Box Canyon near Hagerman, Idaho, to evaluate the ages of the basalts and to use exposure ages to make inferences about the age and mode of formation of the canyon. The U–Th/He ages of the Box Canyon basalts are between 86±12 ka and 130±12 ka (1-sigma errors) and suggest at least two periods of eruption. The ages are similar to a ca. 95 ka Ar–Ar age previously assigned, and distinguish the Box Canyon basalts from nearby ca. 395 ka basalt. Exposure ages of boulders within the canyon at the mouth, head and middle of Box Canyon are 21±1, 19±3 and 48±3 ka; scoured bedrock at the canyon head has an exposure age of 45±5 ka. These data indicate that the canyon was carved before the Bonneville Flood.

Keywords: U–Th/He; cosmogenic helium; Snake River Basalts; Idaho; olivine

* Corresponding author. Now at: Institute for Isotope Geology and Mineral Resources, Department of Earth Sciences, ETH-Zentrum, Clausiusstrasse 25, NW C83.1, 8092 Zurich, Switzerland. Tel.: +41 44 632 37 29; fax: +41 510 486 5496.
E-mail address: aciego@erdw.ethz.ch (S.M. Aciego).

0012-821X/$ - see front matter © 2006 Elsevier B.V. All rights reserved.
doi:10.1016/j.epsl.2006.11.039

1. Introduction

This paper describes the use of the U–Th/He method for obtaining eruption ages of Late Quaternary basalt lavas, and how U–Th/He ages can be combined with ^{3}He exposure ages to reduce uncertainties in the exposure ages and constrain landform development. Recent work has shown that the U–Th/He method gives accurate ages for young garnet, zircon and fayalite with U-rich inclusions [1–3]. These are atypical volcanic minerals and are favorable for dating young volcanic rocks using U–Th/He because of their high uranium concentration. For the U–Th/He method to be a significant new tool for volcanic studies, it needs to be applicable to common phenocryst minerals, and in particular, minerals found within low-potassium basalts. In this work we evaluate the U–Th/He method for dating Quaternary basalts using olivine phenocrysts. We also discuss complementary cosmogenic ^{3}He studies and U–Th/He geochronology, and the practical aspects of identifying the sources of helium isotopes in minerals that have both radiogenic and cosmogenic components.

The lavas we have investigated with the combined U–Th–^{4}He–^{3}He system are basalts of the Snake River Plain, Idaho, which have ages from 100 ka to 3.4 Ma. These samples were chosen for two reasons. The older samples have been dated with the Ar–Ar technique and offer a chance to compare U–Th/He ages with Ar–Ar ages. The younger samples are of interest in evaluating geomorphological models of canyon development in this region, and are sufficiently young that they would be difficult to date accurately with Ar–Ar. In addition, the younger lavas have cosmogenic exposure ages that are similar in magnitude to their eruption ages. These lavas therefore provide an example of a situation where cosmogenic, nucleogenic, and radiogenic helium components can be separated to obtain both eruption ages and exposure ages.

2. Theory

2.1. Magmatic minerals appropriate for U–Th/He dating of basalt

The minerals with the most promising characteristics for dating basalts with U–Th/He are olivine and clinopyroxene [4–6]. Clinopyroxene generally has higher concentrations of U and Th, which should make it the better choice, but its diffusion characteristics appear to be strongly composition-dependent, and thus far, poorly characterized [7]. Helium diffusion in olivine has been studied extensively for various geochemical purposes and shows consistent and favorable behavior regardless of olivine composition and method of analysis [4,5,8]. Largely because of the published consistent high helium retention we have chosen to focus on olivine in this study. The disadvantage of using olivine is that [U] and [Th] (brackets denote concentration) are low, and consequently the amount of radiogenic ^{4}He is relatively small and must be distinguished from initial ^{4}He in the sample. Also, olivine phenocrysts in basalt are embedded in basaltic groundmass that has much higher [U] and [Th] than the olivine. Consequently, ^{4}He from alpha-decay of groundmass U is implanted into the rims of the olivine grains.

To accurately use the ^{4}He content of olivine grains to obtain an eruption age and simultaneously calculate a ^{3}He exposure age, the multiple sources of both ^{4}He and ^{3}He must be taken into account. These various components have been discussed in terms of cosmogenic ages [9–12] and in terms of U–Th/He ages [3], but not together. In the following sections we review the experimental approaches to separating the various contributions to the helium budget of basalt olivine grains, assess their magnitudes, and effects on U–Th/He and cosmogenic exposure ages.

2.2. Isolating radiogenic ^{4}He and cosmogenic ^{3}He in olivine

At the time of eruption, olivine should have ^{4}He and ^{3}He from magmatic and, possibly, atmospheric sources. As the rock ages, the olivine will then accumulate ^{4}He and ^{3}He from *in situ* sources. There will be radiogenic ^{4}He produced by the alpha-decay of U- and Th-series nuclides and a small amount of nucleogenic ^{3}He produced by Li n-alpha reactions associated with the alpha-decay of U- and Th-series nuclides [13]. If the olivine is within about 1 m of the Earth's surface, then there will be both cosmogenic and radiogenic/nucleogenic production of ^{4}He and ^{3}He. The radiogenic and nucleogenic components are proportional to age and U, Th concentration, whereas the cosmogenic component is a measure of the cosmic ray exposure history, which depends on depth below the surface, elevation, latitude, and exposure geometry. In samples with young eruption ages (e.g. <10 ka), surface samples can have substantial cosmogenic ^{3}He, and negligible radiogenic and nucleogenic contributions. However, in samples that are 10^{5}–10^{6} yr old, there can be significant amounts of all components.

The standard procedure for sampling helium in olivine grains is to crush the sample *in vacuo* and

Please cite this article as: S.M. Aciego et al., Combining [^{3}He] cosmogenic dating with U–Th/He eruption ages using olivine in basalt, Earth Planet. Sci. Lett. (2007), doi:10.1016/j.epsl.2006.11.039

measure the [^{4}He], and ^{3}He/^{4}He ratio in the released gas. This measurement is assumed to give the initial helium content and isotopic composition. The crushed sample is then heated *in vacuo* to extract the remaining helium, which is a combination of radiogenic, cosmogenic and nucleogenic components, plus any remaining initial helium not released in the crushing stage.

2.3. Radiogenic ^{4}He

In U–Th/He dating the objective is to measure the radiogenic ^{4}He in the sample that is produced from U and Th residing within the mineral grains. The general equation for the amount of radiogenic ^{4}He in a mineral separate, expressed as function of a measurable quantity, is:

$$^4\mathrm{He}_{\mathrm{rad}} = {}^4\mathrm{He}_{\mathrm{melt}} - {}^4\mathrm{He}_{\mathrm{trap}} - {}^4\mathrm{He}_{\mathrm{c}} \quad (1)$$

Subscripts denote the helium components: *trap* is initial not released upon crushing, *melt* is released in melting after crushing, *c* is produced from cosmogenic sources, and *rad* is produced from radioactive decay of U and Th.

The cosmogenic production rate of ^{4}He at the Earth′s surface at high latitudes is approximately equivalent to the ^{3}He production rate (~ 60 atoms/gm-yr; [14]) and is ~ 3 orders of magnitude lower than the radiogenic production rate, even for the low [U] values of olivine (~ 10 ppb). Therefore, ^{4}He$_c$ can be neglected. If we assume that all of the trapped ^{4}He is released by crushing, then ^{4}He$_{rad}$=^{4}He$_{melt}$. However, if there is still some trapped helium remaining in the sample after crushing, then ^{4}He$_{melt}$ will be higher than ^{4}He$_{rad}$, causing an incorrectly large age to be calculated. This potential problem can be addressed to some degree by first heating the sample at low temperature before melting it. Low-temperature heating should rupture any remaining fluid inclusions and indicate how completely the trapped helium was removed by crushing. The age uncertainty produced by uncertainty in the amount of trapped helium is generally small, but not necessarily negligible, and usually can be adequately assessed using the concentrations and isotopic abundances of the helium released in the crushing, heating, and melting steps (e.g. [15]).

The net gain of radiogenic ^{4}He in basaltic olivine due to α-injection from the groundmass is quite large and can only be addressed by eliminating or greatly reducing its effects. Our approach is to physically abrade the phenocrysts, so that at least 25 μm of the outer portion of every phenocryst is removed prior to analysis [3]. The abraded grains should need no α-injection/ejection corrections. More details on this procedure are given below.

A final issue is that the distribution of U and Th in olivine can be inhomogeneous within individual phenocrysts, from grain to grain, and between subsamples of olivine from a single rock sample. Measured [U] and [Th] in olivine phenocrysts [16] are typically greater than those predicted from olivine/melt distribution coefficients [17], probably because of melt- or micro-mineral inclusions (e.g. metal-oxides, rutile, apatite, or zircon [18]). U and Th mapping of a sampling of grains using an ionprobe can provide insight on the magnitude of the heterogeneity (e.g. [1]). The heterogeneity dictates that U, Th, and ^{4}He concentrations be measured on the same material, and we have designed a sample retrieval system that fulfills this requirement.

2.4. Cosmogenic ^{3}He

Cosmogenic ^{3}He dating of olivine depends on accurately measuring the amount of cosmogenic ^{3}He. The equation for cosmogenic ^{3}He (analogous to Eq. (1) for ^{4}He) is:

$$^3\mathrm{He}_c = \left[\left(^3\mathrm{He}/^4\mathrm{He}\right)_{\mathrm{melt}} - \left(^3\mathrm{He}/^4\mathrm{He}\right)_{\mathrm{trap}} \times \left(\frac{^4\mathrm{He}_{\mathrm{trap}}}{^4\mathrm{He}_{\mathrm{melt}}} \right) - \left(^3\mathrm{He}/^4\mathrm{He}\right)_{\mathrm{rad}} \times \left(\frac{^4\mathrm{He}_{\mathrm{rad}}}{^4\mathrm{He}_{\mathrm{melt}}} \right) \right] \left(^4\mathrm{He}_{\mathrm{melt}}\right) \quad (2)$$

where the total helium released in melting (^{4}He$_{melt}$) is the sum of the trapped and radiogenic (nucleogenic) components. We have expressed the equation in terms of the ratio of the individual components to the total helium released in melting. This allows us to assess the relative magnitude of the trapped and radiogenic components. It should be noted that the ^{4}He$_{trap}$ refers to any ^{4}He left in the same after crushing, ^{3}He/^{4}He$_{trap}$ is the ratio measured in the helium released by crushing, and ^{3}He/^{4}He$_{rad}$ can be estimated from theory.

If the exposure age and the U–Th/He ages are both sufficiently small, it can be assumed that ^{4}He$_{trap}$= ^{4}He$_{melt}$>>^{4}He$_{rad}$ [10]. In this case Eq. (2) reduces to:

$$^3\mathrm{He}_c^* = \left[\left(^3\mathrm{He}/^4\mathrm{He}\right)_{\mathrm{melt}} - \left(^3\mathrm{He}/^4\mathrm{He}\right)_{\mathrm{trap}} \right] \left(^4\mathrm{He}_{\mathrm{melt}}\right) \quad (3)$$

where the asterisk signifies that the assumption has been made that the radiogenic contribution is negligible. If the U–Th/He age is much larger than the exposure age this assumption is unlikely to apply. The error (Δ^3He$_c$) introduced by failing to account for any radiogenic

Please cite this article as: S.M. Aciego et al., Combining [^{3}He] cosmogenic dating with U–Th/He eruption ages using olivine in basalt, Earth Planet. Sci. Lett. (2007), doi:10.1016/j.epsl.2006.11.039

helium that is present can be obtained by subtracting Eq. (2) from Eq. (3) and dividing by $^3He_c^*$, which yields:

$$\frac{\Delta^3He_c}{^3He_c^*} = \frac{\left[\left(^3He/^4He\right)_{rad} - \left(^3He/^4He\right)_{trap}\right] \left(^4He_{rad}\right)}{\left[\left(^3He/^4He\right)_{melt} - \left(^3He/^4He\right)_{trap}\right] \left(^4He_{melt}\right)} \quad (4)$$

where $^4He_{rad}$ is a function of [U+Th] and the closure age. If $^4He_{rad} << ^4He_{melt}$, then there is negligible error as noted above. However, in samples with large enough eruption (closure) ages, where $^4He_{rad}/^4He_{melt}$ is not close to zero, there can be a significant correction. In general, the sign of Δ^3He_c is negative, because $^3He/^4He_{rad} << ^3He/^4He_{trap}$. So an incorrect assumption of negligible radiogenic helium leads to an underestimate of the cosmogenic ^3He. The magnitude of this effect is shown in Fig. 1A using typical [U] and [Th] in olivine. This effect has been discussed previously [12], but only with reference to samples with similar exposure and eruption ages. In situations where the eruption age is many times the exposure age, the error introduced by not accounting for the radiogenic component can be high. If the radiogenic contribution to the ^4He budget is significant, the uncertainty in the ^3He exposure ages can be reduced, especially in olivine samples that are likely to have had negligible diffusive loss of ^4He, by measuring [U] and [Th] concurrently with the exposure age.

When the exposure age is 100 to 1000 times smaller than the U–Th/He age, the radiogenic helium component becomes so large that Eq. (3) can no longer be used to make the correction. Given typical concentrations of Li in olivine and [U] and [Th] in basalt, the error associated with not accounting for the nucleogenic ^3He component can be as high 1–10% (Fig. 1B).

In this situation, typically two rock samples are collected from the site of interest: an exposed sample and a sample shielded from cosmogenic production. Gas extracted from the shielded sample allows the $(^3He/^4He)$ of the combined radiogenic+trapped helium to be measured [19,20]. The cosmogenic helium in the unshielded sample is then calculated from:

$$^3He_c = {}^3He_{melt,unshield} - \left[{}^4He_{melt,unshield} \times \left(^3He/^4He\right)_{melt,unshield}\right] \quad (5)$$

As discussed by [11] this strategy may be the best way of accounting for spatially separated Li and (U, Th).

Similar to radiogenic ^4He, cosmogenic ^3He can be implanted in the olivine grains or ejected into the groundmass, but a net change in the $[^3He]$ depends on

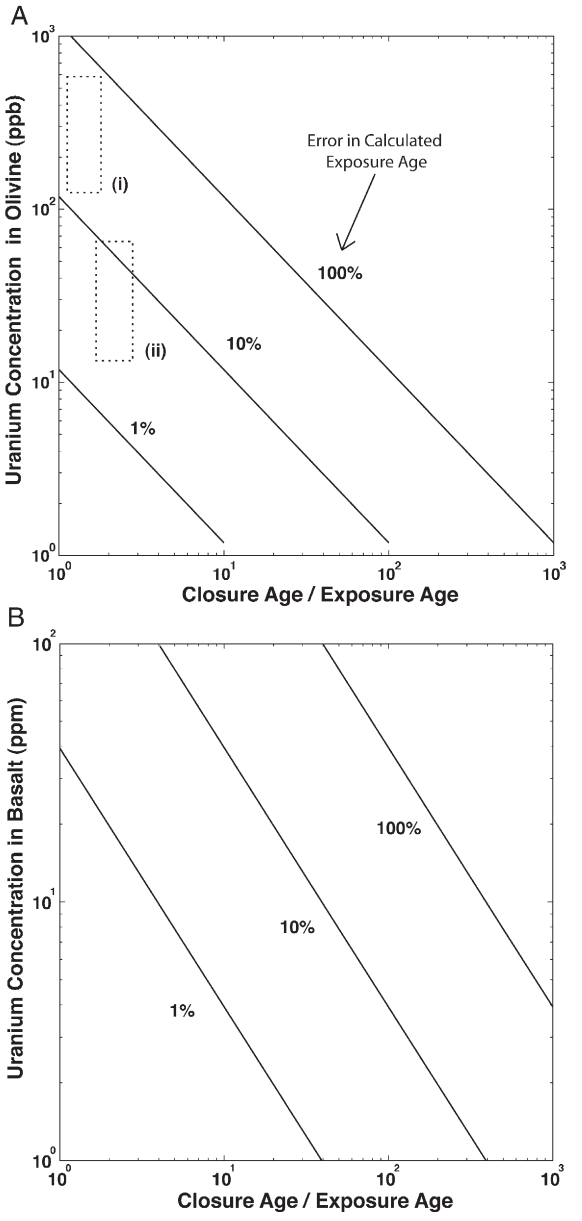

Fig. 1. (A) Errors in the calculated $[^3He]_{cosmogenic}$ due to overcompensating for initial helium using the crush-released $^3He/^4He$ ratio and the heat-released ^4He. Model lines are $([^3He]_{subtracted}/[^3He]_{cosmogenic})$ for various [U] and crystallization/exposure age ratios. The model uses an average trapped helium ratio of 6 R/Ra and a constant Th/U of 3. Box (i) is the range in measured values from [16] and (ii) is the range found in this work. (B) Errors in the calculated $[^3He]_{cosmogenic}$ due to a variable $[^3He]_{nucleogenic}$ component for various [U] concentrations and crystallization/exposure age ratios. The model lines represent a sample with a single Li concentration (3 ppm) and uniform distribution of U and Th within basalt (Th/U of 3); higher Li concentrations will shift the model lines lower.

Please cite this article as: S.M. Aciego et al., Combining [3He] cosmogenic dating with U–Th/He eruption ages using olivine in basalt, Earth Planet. Sci. Lett. (2007), doi:10.1016/j.epsl.2006.11.039

having a different production rate in the olivine from the groundmass (e.g. [11]). In the case of olivine in basalt, the difference in the production rate, calculated from [21], is small enough that the implantation effect is negligible.

3. Geologic setting and sample descriptions

The Snake River Plain is composed of basaltic lavas that trace a path from the Columbia River Basalts of Washington to the Yellowstone Caldera at the Idaho–Montana border. Two sample sites were chosen for testing the (U–Th)/He method on olivine in basalts. The sampled flows have been extensively studied, most recently by [22] who measured high-precision Ar–Ar ages in conjunction with paleomagnetic studies. Because sampling for paleomagnetic work left drill holes in the rock faces, we were able to collect samples from the same location as the paleomagnetic samples. Sample locations are shown in Fig. 2.

Measurements were also made on rock samples from Box Canyon, a 2 km long, amphitheatre-headed tributary canyon to the Snake River, near Hagerman, Idaho. We chose to sample within Box Canyon because of the debate about the volcanic [23,24] and geomorphic history [25,26] of the canyon and our technique allows us to address both exposure history (^{3}He) and eruption ages (U–Th/He).

Over the last ~ 500 ka, basalt flows in the region of Box Canyon are thought to have filled ancestral canyons of the Snake River, diverting the river to the south and west where a new canyon was then cut [23,27–29]. The first event was the eruption of the Madson basalt, which has a K–Ar age of 540 ± 80 ka [30]. Later the Malad Basalt (370 ka), the Thousand Springs Basalt (395 ka), and the Sand Springs Basalt (95 ka) [22] each filled the ancestral Snake River Canyons in this area. Cross-sections of ancestral canyons are visible in the walls of the present Snake River Canyon, where lava fills have been estimated to be at least 60 m and up to 150 m thick, equivalent to the relief of the present day Snake River Canyon (~ 120 m) [31]. Pillow basalts [27] and back-water lacustrine facies [32] are further evidence for the lava dams.

Based on geologic mapping [23], Box Canyon was carved into the Sand Springs Basalt, after it filled a 100 km stretch of the ancestral Snake River canyon at approximately 95 ka [22]. However, recent work [24] suggests that the Sand Springs Basalt did not fill the Snake River Canyon to nearly the same extent as previously inferred, and instead, Box Canyon was carved into the older Thousand Springs Basalt (395 ka) (renamed Basalt of Flat Top Butte), which came from a nearer volcanic vent. It is also suggested [25] that the basalt in the region of Box Canyon appears young because of removal of loess and polishing of volcanic surfaces during the Bonneville mega-flood of 14,500–30 ka [33,34].

The origin of the stubby Box Canyon has recently received attention because of its morphologic similarity to canyons on Mars [26]. Box Canyon currently receives no overland flow and it has been proposed that the canyon was carved by the large (34 m^3/s) spring that emanates from the head of the canyon [25], through progressive upstream retreat of the headwall by spring-driven weathering and erosion processes referred to as "groundwater sapping." A similar conclusion has been

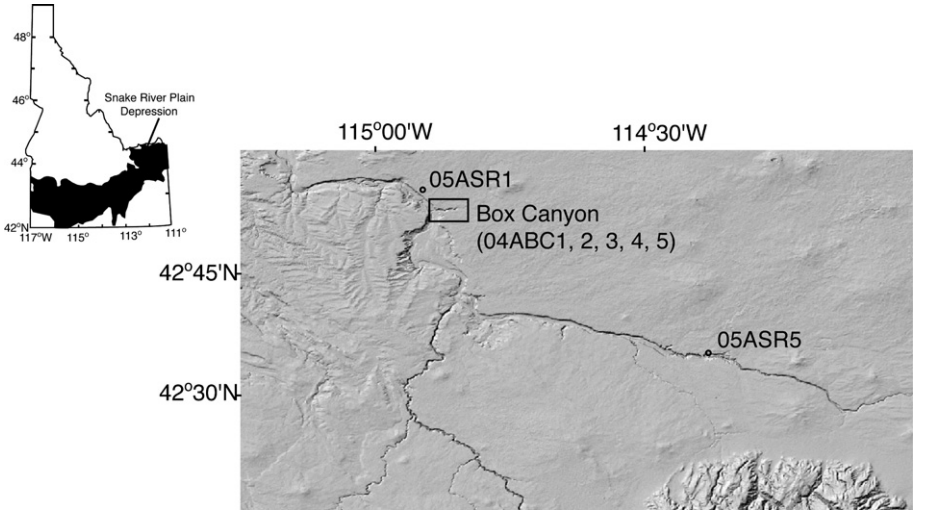

Fig. 2. Location of the Snake River Plain in southern Idaho (modified from [22]) and shaded relief map of south-central Snake River Plain. Samples collected for U–Th/He dating are noted as single locations along the edge of the Snake River, north and southeast of Box Canyon.

Please cite this article as: S.M. Aciego et al., Combining [^{3}He] cosmogenic dating with U–Th/He eruption ages using olivine in basalt, Earth Planet. Sci. Lett. (2007), doi:10.1016/j.epsl.2006.11.039

made for amphitheatre-headed canyons on Mars [35], Box Canyon would therefore be an analog for amphitheatre-headed canyons on Mars, which are also inferred to be formed by sapping. The groundwater sapping model for Box Canyon has recently been questioned [26], because there is little evidence for chemical erosion and insufficient flow from the spring to transport the large boulders (~ 1 m) that line the canyon walls and floor [26]. The alternative model is that a large flood carved the canyon, consistent with the presence of scours at the rim of the canyon head and semicircular talus-free regions along the canyon, indicative of plunge pools.

If Box Canyon was formed by slow progressive retreat of the canyon headwall, we would expect that the canyon is progressively older from the canyon head to the mouth. In this case, it would be expected that large boulders now found near the stream would have older exposure ages near the mouth of the stream and younger ages near the headwall. If a flood formed the canyon in one event, then the exposure age of boulders should be uniform throughout the canyon.

3.1. Sampling strategy

Five samples were taken from Box Canyon (Fig. 3). Sample 04ABC5 was taken from a recent road cut, approximately 30 m below the present land surface. This sample has had negligible cosmogenic exposure and should yield the eruption age of the basalt forming the canyon walls with no complications from cosmogenic effects. The other four samples were collected for combined (U–Th)/He and ^{3}He measurements. At the head of the canyon, we sampled a polished and fluted bedrock surface within a notch carved ~ 2 m into the rim of the canyon head. The depth of scouring is inferred from planar basalt beds that can be traced laterally across the notch. The exposure age of this sample should give the age of formation of the notch by scouring.

Bedrock is exposed in the canyon only at the canyon head. In other locations within the canyon we sampled large boulders that line the canyon floor. Exposure ages of the boulders should record a minimum time for canyon formation, because boulders could presumably detach from the canyon wall and roll to the canyon floor after the canyon was cut. Any shedding of fracture sheets from the boulders will decrease the calculated age. We intentionally sampled boulders that appeared old based on their degree of weathering, and avoided sampling surfaces on the boulders that looked freshly exposed. If the exposure age of any of the boulders is significantly older than that of the scours at the head of the canyon, it would imply that the canyon was cut over a significant duration of time.

We also chose boulders that appeared to be in a geomorphic context that separated them from active boulder-transport processes, and we avoided boulders that were within the stream or active talus slopes. Out of the

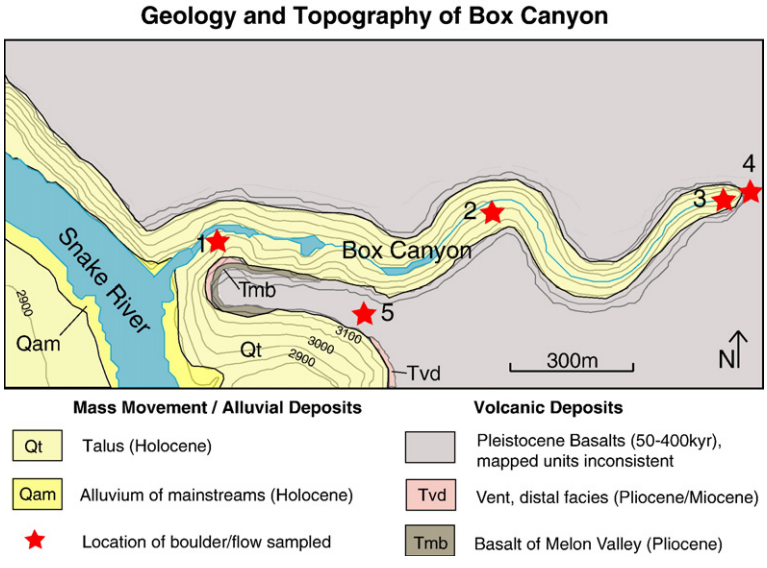

Fig. 3. Mapped geology of the Box Canyon of south-central Idaho, alluvial deposits and older basalts (Tvd, Tmb) following the work of [23] and [24]. Pleistocene basalts' boundaries and relative ages in this area have been mapped differently by different cartographers, therefore we have not drawn the possible boundaries, see text for details. Sample locations are noted, numbers 1–5 correspond to samples 04ABC1–04ABC5 in Table 1. Mapped geology overlies the contours from the *Thousand Springs* USGS topographic quadrangle (contour intervals in feet).

Please cite this article as: S.M. Aciego et al., Combining [^{3}He] cosmogenic dating with U–Th/He eruption ages using olivine in basalt, Earth Planet. Sci. Lett. (2007), doi:10.1016/j.epsl.2006.11.039

three sampled boulders, we hypothesized that boulder sample 04ABC2 is the oldest because it is large (~ 3 m), one side has visible sheeting fractures, it is visibly disconnected and down-slope from the active talus slope, and it is perched on a terrace (presumably a relict fluvial transport surface). For all samples used for cosmogenic dating, the surficial ~ 4 cm of the rock was collected for analysis to maximize the cosmogenic signal.

In order to use the boulder ages as minimum ages of the canyon, we must be able to rule out any cosmogenic exposure that the boulders might have received before the canyon was cut. Therefore, we sampled boulders for which the horizontal and vertical direction of the original basalt flow could be inferred from vesicle distributions. Samples were collected at least 1 m from possible original flow surfaces, as evidenced by direct observation of the original flow surface or inference using the vesicularity and density. The sampled faces had less than a 5° angle with the horizontal to minimize corrections to the production rate.

4. Analytical methods

Approximately 2–5 kg of basalt was crushed and sieved to 400–750 μm. Olivine grains were separated using a combination of magnetic separation and handpicking techniques. Grains were chosen for analysis of they were approximately equidimensional and free of adhering groundmass. Several hundred grains (500–1000 mg) were necessary for each sample to ensure that we had sufficient helium for analysis.

4.1. Sample abrasion to correct for alpha ejection/implantation

Samples were loaded into an alumina vessel and air abraded for 2–3 h [3]. The air abrasion tumbled the grains against each other and the sides of the vessel, removing material in the form of fine powder. Because of the large number of grains in each sample we could not individually determine the thickness of the layer removed from the surface of each grain. Instead, we used a volume approximation and abraded the samples until a full alpha stopping distance was removed. The volume fraction (F_v) that needs to be abraded away in order to ensure that grains of radius r have lost a layer of thickness a, is:

$$F_v = 1 - \frac{(r - a^3)}{r^3} \quad (6)$$

We calculated alpha stopping distances using [36] and a Fo_{50} composition for olivine, resulting in an average stopping distance for the U, Th decay chains of 20 μm. For a minimum grain radius of 200 μm, at least 30% of the volume (or mass) must be removed in order to remove a 20 μm layer from the surface of each grain. There is some complication added by the fact that the highest energy decays in the various chains (e.g. ^{214}Bi, ^{219}Ra, ^{215}Po, ^{211}Bi, ^{216}Po, ^{212}Bi) have stopping distances greater than 20 μm, although all are less than 30 μm. However, because we used the minimum grain radius (ca. 200 μm) instead of the mean grain radius (ca. 275 μm) to calculate F_v, we are assured of eliminating all but a negligible fraction of the ^{4}He implanted in the olivine from the decay of U in the groundmass.

4.2. Trapped helium analysis

After abrasion, the samples were rinsed sequentially in clean methanol, acetone, and ethanol. The samples were then subjected to *in vacuo* crushing using a magnetic mortar and pestle. The magnetic mortar and pestle is based on published designs [37,38], modified to minimize sample contamination — both cross-contamination between samples and contributions of U and Th from the steel. Because of the ultra-low [U] and [Th] in olivine, care must be taken to maintain low blanks during sample processing. To minimize potential cross-contamination, pure, non-magnetic steel was machined into liners for the mortar. The machined liners were then Kolsterized ®, a process that hardens steel from its original hardness of 200 DPN to 1000 DPN (Vicker′s diamond pyramid number) without magnetizing the hardened steel, unlike traditional case-hardening, that would interfere with the operation of the magnet-driven operation of the pestle. The crushers were designed so that samples could be isolated from the mortar and pestle and an active crusher blank measured. Once the blanks were adequately low, the sample was mechanically dropped into the mortar and crushed. Previous studies [15,39,40] have indicated that over-crushing of olivine can result in release of *in situ* produced ^{3}He, so we assume that release of radiogenic ^{4}He from over-crushing is also possible. Therefore, samples were crushed using the optimal number of beats as suggested by [40] of 300 in 5 min, which maximizes the trapped gas release, while minimizing the *in situ* gas release and the accumulated machine blank. Our chosen beat rate is much less than the >1000 beats used where *in situ* produced ^{3}He was observed [39].

4.3. Radiogenic and cosmogenic helium analysis

After crushing, the samples were retrieved and sieved using a 100 μm mesh, and the <100 μm size fraction loaded into clean Pt foil packets. Sieving removes grains

Please cite this article as: S.M. Aciego et al., Combining [^{3}He] cosmogenic dating with U–Th/He eruption ages using olivine in basalt, Earth Planet. Sci. Lett. (2007), doi:10.1016/j.epsl.2006.11.039

that were not fully crushed and may have a trapped component remaining. [U] and [Th] blanks of the 99.99% pure Pt foil were < 1 ppt. Pt foil packets were loaded into a resistance furnace designed for low abundance U–Th/He work. The furnace is capable of achieving temperatures of 1800 °C with sample sizes up to 1.5 g and because the samples were in Pt packets that have a melting temperature of ~ 1800 °C, the samples were fully retrievable for subsequent U and Th analyses. The sample input system thermally isolates the sample during high temperature blank measurements which ensures negligible gas loss prior sample analysis. Gas release was measured at two temperatures: a 300 °C extraction step to release any adsorbed helium and a 1500 °C step to melt and release the cosmogenic ^{3}He and the radiogenic ^{4}He. Samples were heated to the desired temperature over 15 min, held at that temperature for 30 min and cooled for 15 min. Periodically, we measured a third 1600 °C step to check that gases were fully released.

After extraction, the gas was purified on a series of getters and adsorbed onto a charcoal trap held at 8 K, the activated charcoal trap has a 100% He trapping efficiency. The helium was released into the mass spectrometer by heating the charcoal trap to 30 K. The isotopic and abundance analyses were made on a VG5400 mass spectrometer equipped with a Faraday cup and an electron multiplier operated in pulse counting mode. Abundance measurements were calibrated using an aliquot of air and a reference sample of helium (R=2.4 Ra) run periodically during the course of the sample analyses. Blanks were run for each sample prior to crushing and the ^{4}He varied from 0.5 to 2.6×10^{-10} cc STP. The long-term crushing blank average is $0.8\pm0.4\times10^{-10}$ cc STP. Furnace blanks were measured at the 300 °C and 1500 °C temperature steps prior to each sample and the ^{4}He varied from 0.5 to 1.3×10^{-10} cc STP, the long-term furnace average is $0.8\pm0.3\times10^{-10}$ cc STP.

4.4. U and Th analysis

After the total gas extraction, the sample packets are retrieved and the fused sample is removed from the foil. The fused olivine beads are not visibly reacted with the Pt foil, allowing easy removal. The sample is dissolved in an HNO_3–HF–$HCLO_4$ acid solution. Dissolutions were checked for completeness and formation of any fluorides by centrifuging, and treating fluorides with an HCl–Boric acid solution. Aliquots of the solutions were spiked with ^{229}Th and ^{233}U, unspiked aliquots were analyzed for ^{234}U/^{238}U and ^{230}Th/^{232}Th. Isolation of U and Th was accomplished using Tru-Spec® column resin following established procedures [41].

Uranium and thorium concentration and isotopic measurements were measured at Woods Hole

Table 1
Description of samples

Site	Sample	Altitude (m)	Lat., N	Lon., W	Description	Shielding, azimuth: inclination (degrees)
Previously dated flows						
Malad Basalt	05ASR1		42.84027	114.88821	Olivine, plagioclase phyric basalt. Collected samples 2–3 m from top of flow, next to drill core holes, corresponding to SR011 from [22].	N/A
Idaho Group Qi10	05ASR5		42.60212	114.39787	Plagioclase phyric, olivine poor, massive basalt. Collected 2–3 m from top of flow, next to drill core holes, corresponding to SR01 from [22].	N/A
Box Canyon flows and boulders						
Boulder 1	04ABC1	864	42.70724	114.8206	Olivine, plagioclase phyric massive basalt. Micro-vesicles, but no flow structures indicative of flow surface. Boulder located 3 m above current stream level.	0: 0, 100: 6, 220: 22, 235: 6, 275: 6, 281: 10
Boulder 2	04ABC2	886	42.70784	114.81278	Plagioclase phyric, olivine poor, massive basalt. Sample collected 2 m from possible top of flow. Boulder located at least 3 m above current stream level.	0: 0, 100: 10, 105: 28, 250: 5, 255: 23, 325: 27
Boulder 3	04ABC3	922	42.70796	114.80466	Massive basalt, microphenocrystic olivine. Boulder located at stream level.	0: 0, 65: 12, 160: 24, 230: 5, 345: 24
Top flow	04ABC4	978	42.70833	114.80292	Vesiculated olivine phyric basalt exposed at top of canyon. Flute marks indicative of heavy water flow.	0: 24, 90: 0, 180: 11, 270: 0
Bottom flow	04ABC5	947	42.70544	114.81915	Olivine phyric basalt. Collected sample 30 m below top of sequence flows.	N/A

Please cite this article as: S.M. Aciego et al., Combining [^{3}He] cosmogenic dating with U–Th/He eruption ages using olivine in basalt, Earth Planet. Sci. Lett. (2007), doi:10.1016/j.epsl.2006.11.039

Oceanographic Institution by isotope dilution on a ThermoFinnegan Element 2 ICPMS in pulse counting mode. Samples were introduced to the instrument using a CETAC Aridus desolvation system. Prior to each analysis a scan of the mass spectrum from mass 227 to mass 240 is measured to evaluate background. Each sample measurement was made in triplicate and bracketed by measurement of an acid blank and standard NBS 960. Mass fractionation was corrected using the $^{235}U/^{238}U$ ratio of NBS960. The uncertainty in the measured concentrations, based upon triplicate measurements, varies from 0.75 to 1.5% in Th and 0.5–0.75% in U.

U and Th isotopic measurements were made on a ThermoFinnegan Neptune MC ICPMS. Thorium isotopic analyses were made statically, measuring ^{232}Th on a Faraday cup and ^{230}Th on the RPQ channel using an ETP SEM. Using the RPQ on the ThermoFinnigan Neptune, the abundance sensitivity at 85% transmission was ~ 50 ppb over 2 amu, resulting in a tail correction of ^{232}Th on ^{230}Th of ~ 0.3% for a ratio of 1.5×10^5. To correct for both instrumental mass fractionation between masses 230 and 232 and the relative difference in the efficiency of the Faraday and SEM detectors, Th isotopic measurements were corrected based upon a linear interpolation of the $^{232}Th/^{230}Th$ measured in the UCSC ThA between each sample, and normalized to a value of 170,765 [42]. Sensitivity based on U with a normal spray chamber (wet plasma) and standard nickel cones expressed as ion yield is approximately 0.1%. Linear range of the SEM is less 20 k CPS. Best linearity

Table 2
Sample weights, before and after abrasion, U, Th, He concentrations and isotopic compositions

Sample	Pre abr wt. (g)	Post abr wt. (g)	Melt wt. (g)	[U], ppb	[Th], ppb	$[^{230}Th/^{232}Th]_{act}$	$[^{234}U/^{238}U]_{act}$	$[^4He], \times10^{-5}$ nmol/g	$[^3He], \times10^{-9}$ nmol/g
04ABC1	0.9501	0.5401	0.50820						
Crush								2.034±170	0.1±1
300 °C								0.263±13	0.1±1
1500 °C				24.93±19	68.34±70	0.92±1	1.00±1	2.234±182	7.4±3
04ABC2	1.0021	0.6302	0.59315						
Crush								2.757±223	0.1±1
300 °C								4.104±446	0.1±1
1500 °C				73.47±44	95.68±96	1.94±1	1.00±1	4.131±337	17.7±5
04ABC2(2)	0.8489		0.83261						
Crush								9.257±754	8.6±7
1500 °C								87.999±720	18.5±5
04ABC3	1.4777	0.9656	0.73190						
Crush								0.423±5	0.1±1
300 °C								0.363±5	0.1±1
1500 °C				42.07±27	68.95±74	1.38±1	1.00±1	3.009±283	7.3±2
04ABC4	0.6429	0.3305	0.30960						
Crush								0.000±5	0.1±1
300 °C								0.267±5	0.1±1
1500 °C				54.89±33	163.84±165	0.85±1	1.00±1	3.862±494	17.8±5
04ABC5	1.2431	0.8932	0.75260						
Crush								0.486±40	0.1±1
300 °C								0.437±5	0.1±1
1500 °C				47.12±33	136.47±137	0.87±1	1.01±1	3.545±329	0.1±1
05ASR1	1.1141	0.7516	0.73331						
Crush								1.512±125	0.1±1
300 °C								0.335±5	0.1±1
1500 °C				19.13±13	44.01±47	1.26±1	1.02±2	6.131±555	0.1±1
05ASR5	1.3526	0.8612	0.82042						
Crush								0.308±27	0.1±1
300 °C								0.580±27	0.1±1
1500 °C				20.98±13	66.14±68	0.97±1	0.99±1	64.108±5232	0.1±1
TML				10403±649	28948±8380	1.08±1	1.00±1		

Helium values reported are blank corrected using the blank measured directly before each sample measurement, 1600 °C extractions are not reported because no further gas was released on re-extraction.
Activity ratios calculated using $\lambda_{230}=9.195\times10^{-6}$ yr^{-1}, $\lambda_{232}=4.948\times10^{-11}$ yr^{-1}, $\lambda_{234}=2.826\times10^{-6}$.
Errors are reported as 2S.D. for U, Th and He.
^3He values of 0.1 +/− 0.1 are at blank levels.
TML is Table Mountain Latite.

Please cite this article as: S.M. Aciego et al., Combining [^3He] cosmogenic dating with U–Th/He eruption ages using olivine in basalt, Earth Planet. Sci. Lett. (2007), doi:10.1016/j.epsl.2006.11.039

is achieved by matching samples and standards to within a factor of 2. Dead time was measured to be 20 ns and is software corrected. Replicate measurements of TML (Table Mountain Latite) are in equilibrium within analytical uncertainty verifying reliability in both [U] and [Th] concentration and $^{232}Th/^{230}Th$ isotopic measurements. Uranium isotopic analyses were made statically measuring ^{238}U and ^{235}U on Faraday cups and ^{234}U on an ETP SEM. NBS U010 was measured between each sample to determine SEM/Faraday gain. For these samples ($^{234}U/^{238}U$)=1 within error, using an equilibrium $^{234}U/^{238}U$ of 54.48 ppm [43].

5. Data reduction and age calculations

5.1. Concentrations and isotopic composition of He, U and Th

Sample weights, before and after abrasion, helium concentrations, and U, Th concentrations and isotopic compositions of the seven samples are shown in Table 2. The largest uncertainties in the radiogenic ^4He concentrations are due to the blank correction because of the low abundance of ^4He in the samples. We evaluate the possibility of *in situ* produced helium lost in crushing [15] by comparing the amount of ^3He released in crushing to that released by melting. The exposed samples showed no ^3He released by crushing despite significant amounts released by melting. We infer that there is negligible loss of *in situ* helium during the crushing stage.

We do not correct the ^3He concentration for a magmatic component because the relative abundance of trapped helium to helium released in melting is low, as expected for a basalt that likely flowed over a large distance during eruption and largely degassed. As discussed in Section 2 and [16], correcting the ^3He released in heating using the $^3He/^4He$ ratio measured in crushing can drastically over-correct the ^3He concentration and force an underestimation of the exposure age. Furthermore, we do not need to account for nucleogenic ^3He because the difference between the exposure and the eruption age is sufficiently small (Fig. 1B).

5.2. U-series disequilibrium and ages

Variations from secular equilibrium in the U and Th decay chains must be taken into account when calculating the U–Th/He age for samples less than 1 million years old, otherwise the calculated age can differ from the true age by as much as 50% [1,2]. Because our samples are greater than 20 ka, we can neglect Ra disequilibrium and use the age equation:

$$^4\mathrm{He} = P_{\mathrm{se}}(U,\mathrm{Th})(1+F_{\mathrm{dis}}) \tag{7}$$

where

$$P_{\mathrm{se}}(U,\mathrm{Th}) = 7(^{235}U)(e^{\lambda_{235}t}-1) + 6(^{232}\mathrm{Th}) \times (e^{\lambda_{232}t}-1) + 2(^{238}U)(e^{\lambda_{238}t}-1) \tag{8}$$

is the production rate of ^4He expected for a system at U series radioactive equilibrium, and

$$F_{\mathrm{dis}} = \frac{1}{P_{\mathrm{se}}(U,\mathrm{Th})}\left\{6D_{230}\left(\frac{\lambda_{238}}{\lambda_{230}}\right)(^{238}U)e^{\lambda_{238}t}(1-e^{-\lambda_{230}t}) + 6(^{238}U)\lambda_{238}e^{\lambda_{238}t}\left[\left(\frac{1}{\lambda_{238}}\right)(1-e^{-\lambda_{238}t}) + \left(\frac{1}{\lambda_{230}}\right)(e^{-\lambda_{238}t}-1)\right]\right\} \tag{9}$$

is the correction factor for departures from equilibrium. The terms ^4He, ^{235}U, ^{232}Th, and ^{238}U refer to

Table 3
Calculated U-Th/He ages, and comparison of U-Th/He, Ar-Ar, and cosmogenic ^3He ages

Sample	U	Th (nmol/g)	He, $\times 10^{-5}$	D_{230}	Equilibrium [a] U–Th/He Age (ka)	Disequilibrium U–Th/He Age (ka)	1σ [b]	^3He Cosmogenic Exposure Age (ka)	1σ	Ar–Ar Age (ka) (from [22])	2σ
04ABC1	0.104	0.293	2.234	0.59	100	118	11	21	1		
04ABC2	0.304	0.414	4.131	0.61	81	94	9	48	3		
04ABC2(2)								51	3		
04ABC3	0.175	0.297	3.009	0.30	96	130	12	19	3		
04ABC4	0.229	0.707	3.862	0.62	76	86	12	45	5		
04ABC5	0.196	0.586	3.710	0.54	86	100	10				
05ASR1	0.079	0.190	6.131	0.75±0.25		401	42			373	12
05ASR5	0.088	0.284	64.108	0.75±0.25		3255	260			3400	60

[a] Calculated ages based on D_{230}=1.

[b] Errors are calculated by running Monte Carlo simulations using a Gaussian distribution in the errors σ_{He}, σ_U, σ_{Th}, $\sigma_{D_{230}}$. Unless D_{230}=1, then $\sigma_{D_{230}}$ values based on a Gaussian distribution of possible D_{230} values with a mean of 0.75.

Please cite this article as: S.M. Aciego et al., Combining [^3He] cosmogenic dating with U–Th/He eruption ages using olivine in basalt, Earth Planet. Sci. Lett. (2007), doi:10.1016/j.epsl.2006.11.039

concentrations, λ′s are decay constants, and D_{230}=^{230}Th/^{238}U activity ratio at the time of helium closure. Calculated U–Th/He ages using the equilibrium age equation and Eq. (8) are shown in Table 3, along with the Ar–Ar ages.

The isotopic composition of the Snake River Plain Basalts olivine separates is plotted on the ^{230}Th/^{232}Th–^{238}U/^{232}Th activity diagram [44] (Fig. 4). The distance the datum plots from the equiline is defined by the initial U–Th disequilibrium at the time of eruption and the age. The oldest sample (05ASR5), which is 3.4 Ma, plots directly on the equiline, consistent with the crystallization age being much larger than the half-life of ^{230}Th. Sample 05ASR1 is close to the equiline, but does not lie on it, an indication that the sample is too young to have ingrown all deficiency in ^{230}Th. This observation is consistent with the published Ar–Ar age (370 ka). In contrast, the samples from Box Canyon lie far off the equiline, as expected considering their younger ages. These samples fall on a general trendline, a "pseudo isochron." Noted on Fig. 4 are two possible isochrons that bound the Box Canyon data corresponding to apparent crystallization ages of 194 ka and 78 ka. The U–Th/He ages should be and are consistent with these approximate U–Th ages.

5.3. Production rate of in situ ^{3}He and ages

The production rate of cosmogenic ^{3}He in olivine has been extensively studied and calibrated [10,45–48]. We use the equatorial, sea level average value of 103±4 at g^{-1} yr^{-1} and scale it using the equations of [14] modified by [49,50] based on the latitude, altitude, shielding, and slope of each sample as described in Table 1. The shielding geometry for each sample is not simple: neither rectangular nor triangular obstructions adequately describe the geometry. However, in the case of the highest possible shielding, which applies to sample 04ABC2, assuming a simple rectangular obstruction across the horizon results in a decrease in the total production rate by only 4.4%. The alternative calculation (triangular obstructions) reduces the change in the production rate to less than 1%. Both calculations assume that the shielding geometry has remained the same as the current sample position. For this reason, we have instead folded the possibility of shielding into the error in the production rate for each sample. Using the simple formula $[^3\mathrm{He}]_c = P^* t$, we calculate the exposure ages of the boulders and scours at the head of the canyon given in Table 3.

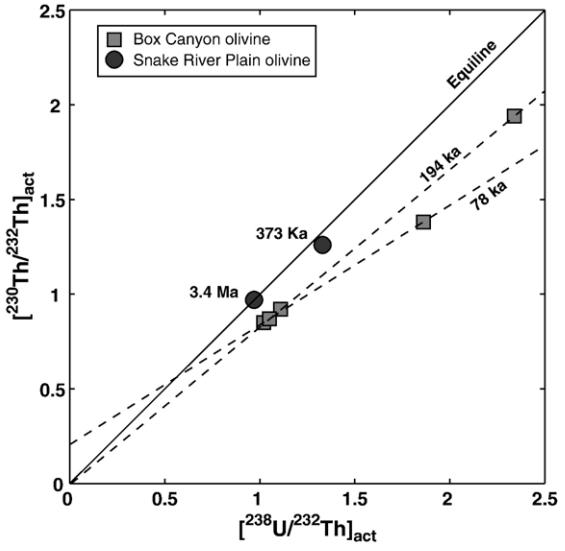

Fig. 4. ^{230}Th/^{232}Th–^{238}U/^{232}Th activity diagram of the Snake River Plain basalt olivine separates. Two "pseudo-isochrons" are drawn for the olivine separates taken from different sample locations noted in Fig. 3.

6. Results and discussion

6.1. Geochronology of basalt using U–Th/He on olivine

The U–Th/He age obtained from the olivine of sample ASR5 is 3255±260 ka (1σ), which compares to the Ar–Ar plateau age of 3400±60 ka (2σ), and an Ar–Ar isochron age of 3410±180 ka from [22]. The U–Th/He age is about 4% lower than the Ar–Ar age but within the 1σ error limits of the U–Th/He age. For sample ASR1, the U–Th/He age is 401±42 ka, the Ar–Ar plateau age is 373±12 ka, and the Ar–Ar isochron age is 369±16 ka. In this case the U–Th/He age is slightly older. For these samples, which have reasonably high K contents, the Ar–Ar method gives a more precise age. The data demonstrate that the U–Th/He method gives accurate ages on samples up to ca. 3.5 Ma, which suggests that diffusive loss of helium from olivine is insignificant up to this age range.

The analytical procedures for U–Th/He dating probably limit the precision of the determined ages to about ±5% to ±10% at the 1-sigma level, largely due to limitations on the measurements of helium concentration [1]. The accuracy of the calculated ages can also suffer for samples in the >300 ka range due to U–Th disequilibrium. The U–Th disequilibrium remains a problem in determining ages precisely for samples in the age range 300 ka–2 Ma because the state of ^{230}Th/^{238}U equilibrium at the time of eruption cannot be measured directly on the sample in the way it can be for younger samples. For samples as old as ~ 3 Ma, the uncertainty becomes a

Please cite this article as: S.M. Aciego et al., Combining [^{3}He] cosmogenic dating with U–Th/He eruption ages using olivine in basalt, Earth Planet. Sci. Lett. (2007), doi:10.1016/j.epsl.2006.11.039

relatively small fraction of the age and can be up to 4% [3], although under usual circumstances it is likely to be 1–2%. For samples 300–800 ka the uncertainty is a maximum. In extreme cases, where the D_{230} value is between 0 and 0.2, the error could be as high as 12%. However, given that mineral separates within continental basalts have been observed to fractionate less than 20% from whole rock values, a realistic error would be 2–5%. Given a nominal 1-sigma uncertainty in the age calculation of 9% due to analytical uncertainties, the resulting *total uncertainty* (analytical plus U–Th disequilibrium) in the age is typically about 10 to 12% for samples within this age range. This uncertainty is reflected in the high error in the age of sample ASR1. Although this level of precision is low by comparison to the best that can be achieved in geochronology, it is likely to be useful in the age range of 50 ka–3000 ka, especially for basalt lavas that are poor in potassium, and for some that are erupted in continental areas where there are issues with contamination or Ar inheritance, or where, the rocks have low radiogenic ^{40}Ar (e.g. [51] and [22], samples sr19 and sr31). The two Ar–Ar dated samples from [22] that we have chosen for comparison, gave good Ar–Ar plateaus, and hence have small uncertainties. However, even these samples have enough structure in the Ar release patterns that it is possible the Ar–Ar ages contain artifacts at the level of 10% of the age. Other samples measured by [22] in the same age range have much more ragged Ar release patterns, and even where the reported analytical uncertainty is a few percent, individual step release ages vary by 20% of the age. Differences between plateau ages and isochron ages are also up to 20% of the age. In general it is difficult to establish the age of young basaltic lavas with confidence (e.g. [51,52]) and the U–Th/He method could be a useful addition to existing geochronological methods.

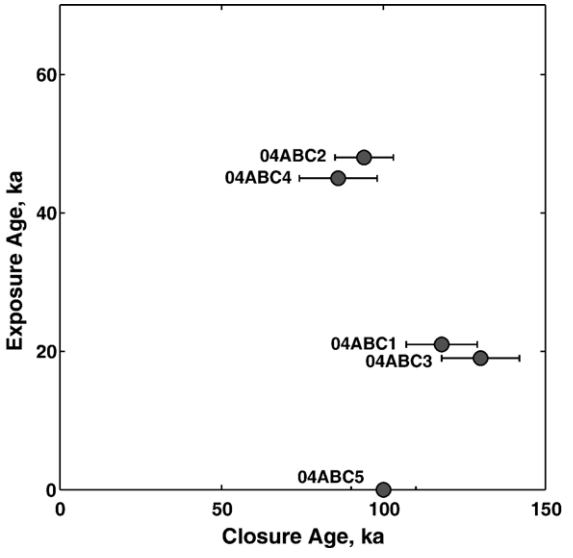

Fig. 5. Plotted ^{3}He exposure ages and U–Th/^{4}He closure ages determined on samples from Box Canyon, Idaho.

6.2. Box Canyon U–Th/He ages

The U–Th/He ages for the Box Canyon basalt samples vary from 86±12 to 130±12 ka. Sample 04ABC4 is from the top of the ca. 50 meter-thick section of basalt flows exposed at the head of the canyon, and its age is 86± 12 ka. Sample 04ABC5 is from about 30 m (and at least 2 flow units) stratigraphically below 04ABC4 and gives the age of 100±10 ka. These data suggest that the flows exposed in the canyon represent a series of eruptions that spanned a period of about 30 ka. The U–Th/He ages of one of the boulders (94±9 ka) is close to the age of the top flow unit from the head of the canyon, whereas the age of the other boulder (118±11 ka) is closer to the age of the flow from lower in the section.

Our eruption ages indicate that the basalt of Box Canyon is not the ca. 395 ka Thousand Springs Basalt. The ages are more compatible with the previously determined K–Ar age of 95 ka for the Sand Springs Basalt, as originally mapped by [23]. Furthermore, the relative uniformity of ages from samples separated by ~ 30 m in stratigraphy (04ABC4 to 04ABC5) suggests that there was a depression with significant relief into which the basalt flowed. This supports the hypothesis that Sand Springs Basalt filled an ancestral Snake River Canyon, as there are no other apparent mechanisms for creating such relief in the Snake River Plain. The time between the Sand Springs and later canyon filling episodes and the depths of the ancestral canyons indicate that the Snake River has been competent to incise at rapid rates of at least several millimeters per year, rates that are usually associated with rapidly uplifting landscapes.

The basalt fills of the ancestral canyons are particularly important because, where intersected by the present-day Snake River Canyon, they are associated with some of the largest springs in North America [53], fed by an aquifer that underlies most of the Snake River Plain. The springs are thought to occur at basaltic canyon fills because of their high permeability and storage capacity [28] and one such spring emanates from the headwall of Box Canyon.

6.3. Box Canyon cosmogenic ^{3}He ages

The ^{3}He cosmogenic ages of the boulders in the canyon range from 19±3 to 50±3 ka. The replicate

Please cite this article as: S.M. Aciego et al., Combining [^{3}He] cosmogenic dating with U–Th/He eruption ages using olivine in basalt, Earth Planet. Sci. Lett. (2007), doi:10.1016/j.epsl.2006.11.039

analyses of sample 04ABC2 (48±3 ka and 51±3 ka) indicate that the estimated analytical uncertainties are realistic and hence there are substantial differences in the exposure ages of the boulders. The scoured notch at the head of the canyon has an exposure age of 45±5 ka, similar to the 50±3 ka age of the boulder located midway between the canyon head and mouth. The two other boulders, one near the mouth and one at the head of the canyon, give ages of 19±3 and 21±1 ka. None of the exposure ages are as old as the eruption ages of the basalt sequence (Fig. 5). While the number of samples is small, none of the boulders are significantly older than the scours at the head of the canyon, despite the fact that we intentionally sampled boulders that appeared to be old. This suggests that the canyon might have been carved in a relatively short time period, at approximately 45–50 ka, which is consistent with the flood hypothesis of [26], and probably incompatible with the groundwater sapping hypothesis of [25]. The exposure date of the scoured notch at the head of Box Canyon (sample 04ABC4) indicates that Box Canyon is older than the Bonneville Flood, contrary to the recent mapping of [24]. This conclusion is also supported by the flood modeling of [54] who infer that the flood was contained within the Snake River Canyon in the region of Box Canyon, and therefore could not have cut Box Canyon.

7. Conclusions

The results presented here demonstrate that the U–Th/He method can be applied to olivine phenocrysts to obtain accurate ages of basalt lavas with ages between 80 and 3500 ka with a nominal 1-sigma uncertainty of ±10%. The method as we have employed it relies on abrading the olivine grains to eliminate to the effects of He implantation from the decay of groundmass U, and improvements in the analytical techniques. Critical improvements are a low-blank crushing system with a hardened steel liner to prevent cross-contamination between samples, and a retrieval system so that U and Th concentrations can be measured on the same olivine grains that are measured for helium concentration.

The significance of dating a series of basaltic eruptions from the Snake River Plain using the U–Th/He method on olivine phenocrysts is twofold. First, this investigation shows that a common mineral in basalts, olivine, can be used to determine eruption ages. Given the U and Th we have measured, olivine as young as 25 ka can be dated. The upper age range is limited by the diffusivity of helium in olivine, which can be further quantified by diffusion experiments, but appears greater than 3500 ka. For dating the time period from the limit of radiocarbon dating (ca. 40 ka) up to a few million years, the U–Th/He method may be particularly useful for basaltic rocks with low potassium, submarine basalts, those with inherited Ar, incomplete degassing, or other issues affecting the Ar–Ar approach.

This work also shows that ^{3}He cosmic ray exposure ages and U–Th/He ages can be investigated simultaneously. Previous investigations of exposure histories using ^{3}He without concurrent U–Th/^{4}He measurements are limited by assumptions about the contributions of radiogenic ^{4}He in the pre-exposure history of the rocks. When the total U–Th–^{4}He–^{3}He system is investigated the uncertainties in both ages can be specified with more certainty.

Acknowledgements

This work was funded by NASA Astrobiology Institute under grant NASA NAI02-0024-0006 and by the Director, Office of Science, Office of Basic Energy Sciences, U.S. Department of Energy under Contract DE-AC02-05CH11231. We thank Ken Farley and an anonymous reviewer for their helpful comments. We thank Gina Pecht for her invaluable laboratory assistance.

References

[1] S. Aciego, B.M. Kennedy, D.J. DePaolo, J.N. Christensen, I. Hutcheon, U–Th/He age of phenocrystic garnet from the 79 AD eruption of Mt. Vesuvius, Earth Planet. Sci. Lett. 216 (2003) 209–219.

[2] K.A. Farley, B.P. Kohn, B. Pillans, The effects of secular disequilibrium on (U–Th)/He systematics and dating of Quaternary volcanic zircon and apatite, Earth Planet. Sci. Lett. 201 (2002) 117–125.

[3] K. Min, P.W. Reiners, J.A. Wolff, R. Mundil, R.L. Winters, (U–Th)/He dating of volcanic phenocrysts with high U–Th inclusions, Jeniez Volcanic Field, New Mexico, Chem. Geol. 227 (2006) 223–235.

[4] S.R. Hart, He diffusion in olivine, Earth Planet. Sci. Lett. 70 (1984) 297–302.

[5] T.W. Trull, M.D. Kurz, W.J. Jenkins, Diffusion of cosmogenic He-3 in olivine and quartz — implications for surface exposure dating, Earth Planet. Sci. Lett. 103 (1991) 241–256.

[6] T.W. Trull, M.D. Kurz, Experimental measurements of He-3 and He-4 mobility in olivine and clinopyroxene at magmatic temperatures, Geochim. Cosmochim. Acta 57 (1993) 1313–1324.

[7] H.J. Lippolt, E. Weigel, He-4 diffusion in Ar-40 retentive minerals, Geochim. Cosmochim. Acta 52 (1988) 1449–1458.

[8] D.L. Shuster, K.A. Farley, J.M. Sisterson, D.S. Burnett, Quantifying the diffusion kinetics and spatial distributions of radiogenic He-4 in minerals containing proton-induced He-3, Earth Planet. Sci. Lett. 217 (2004) 19–32.

[9] R.P. Ackert, B.S. Singer, H. Guillou, M.R. Kaplan, M.D. Kurz, Long-term cosmogenic He-3 production rates from Ar-40/Ar-39 and K-Ar dated Patagonian lava flows at 47 degrees S, Earth Planet. Sci. Lett. 210 (2003) 119–136.

Please cite this article as: S.M. Aciego et al., Combining [^{3}He] cosmogenic dating with U–Th/He eruption ages using olivine in basalt, Earth Planet. Sci. Lett. (2007), doi:10.1016/j.epsl.2006.11.039

[10] M.D. Kurz, Insitu production of terrestrial cosmogenic helium and some applications to geochronology, Geochim. Cosmochim. Acta 50 (1986) 2855–2862.
[11] K.A. Farley, J. Libarkin, S. Mukhopadhyay, W. Amidon, Cosmogenic and nucleogenic ^{3}He in apatite, titanite, and zircon, Earth Planet. Sci. Lett. 248 (2006) 451–461.
[12] A.J. Williams, F.M. Stuart, S.J. Day, W.M. Phillips, Using pyroxene microphenocrysts to determine cosmogenic He-3 concentrations in old volcanic rocks: an example of landscape development in central Gran Canaria, Quat. Sci. Rev. 24 (2005) 211–222.
[13] B.A. Mamyrin, I.N. Tolstikhin, Helium isotopes in nature, Elsevier, New York, 1984. 273 pp.
[14] D. Lal, Cosmic-ray labeling of erosion surfaces — in situ nuclide production-rates and erosion models, Earth Planet. Sci. Lett. 104 (1991) 424–439.
[15] P.H. Blard, R. Pik, J. Lave, D. Bourles, P.G. Burnard, R. Yokochi, B. Marty, F. Trusdell, Cosmogenic He-3 production rates revisited from evidences of grain size dependent release of matrix-sited helium, Earth Planet. Sci. Lett. 247 (2006) 222–234.
[16] P.H. Blard, J. Lave, R. Pik, X. Quidelleur, D. Bourles, G. Kieffer, Fossil cosmogenic He-3 record from K–Ar dated basaltic flows of Mount Etna volcano (Sicily, 38 degrees N): evaluation of a new paleoaltimeter, Earth Planet. Sci. Lett. 236 (2005) 613–631.
[17] B.J. Wood, J.D. Blundy, J.A.C. Robinson, The role of clinopyroxene in generating U-series disequilibrium during mantle melting, Geochim. Cosmochim. Acta 63 (1999) 1613–1620.
[18] K. Kothay, C. Szabo, V.V. Sharygin, K. Torok, Silicate melt inclusion study on olivine phenocrysts and clinopyroxene microphenocrysts in the Hegyestu Basalt, Bakony–Balaton Highland, Hungary, XVI ECROFI European Current Research on Fluid Inclusions, Porto, 2001.
[19] T.E. Cerling, R.J. Poreda, S.L. Rathbum, Cosmogenic He-3 and Ne-21 age of the Big Lost River flood, Snake River Plain, Idaho, Geology 22 (1994) 227–230.
[20] R.P. Ackert, M.D. Kurz, Age and uplift rates of Sirius Group sediments in the Dominion Range, Antarctica, from surface exposure dating and geomorphology, Glob. Planet. Change 42 (2004) 207–225.
[21] J. Masarik, R. Reedy, Monte Carlo simulation of in-situ-produced cosmogenic nuclides, Radiocarbon 38 (1996) 163–164.
[22] L. Tauxe, C. Luskin, P. Selkin, P. Gans, A. Calvert, Paleomagnetic results from the Snake River Plain: contribution to the time-averaged field global database, Geochem. Geophys. Geosyst. 5 (2004).
[23] H.R.Covington, J.N.Weaver, Geologic map and profiles of the north wall of the Snake River Canyon, Thousand Springs and Niagara Springs quadrangles, Idaho, US Geological Survey Miscellaneous Investigations 1991, pp. Map I-1947-C.
[24] V.S. Gillerman, J.D. Kauffman, K.L. Othberg, Geologic map of the Thousand Springs Quadrangle, Gooding and Twin Falls Counties, Idaho, Idaho Geological Survey, Moscow, Idaho, 2006.
[25] H.T. Stearns, Origin of the large springs and their alcoves along the snake river in southern Idaho, J. Geol. 44 (1936) 429–450.
[26] M.P. Lamb, A.D. Howard, J. Johnson, K. Whipple, W.E. Dietrich, J.T. Perron, Can springs cut canyons into rock? J. Geophys. Res. Planets 111 (2006).
[27] H.E. Malde, History of the Snake River canyon indicated by revised stratigraphy of the Snake River Group near Hagerman and King Hill, Idaho Us Geological Survey Professional Paper, 1971, p. 20.
[28] H.R. Covington, W.R.L., W.J.N., Ancestral canyons of the Snake River; geology and geohydrology of canyon-fill deposits in the Thousand Springs area, south-central Snake River Plain, Idaho, Geological Society of America Rocky Mountain Section Annual Meeting, Composite Field Guide, Trip 7, Boise, Idaho, 1985, p. 30.
[29] H.E. Malde, Quaternary geology and structural history of the Snake River Plain, Idaho and Oregon, in: M. R.B. (Ed.), Quaternary Nonglacial Geology: Conterminous U.S., The Geology of North America K-2, Geological Society of America, Boulder, CO, 1991, pp. 251–281.
[30] R.L. Armstrong, W.P. Leeman, H.E. Malde, K–Ar dating, quaternary and Neogene volcanic-rocks of Snake River Plain, Idaho, Am. J. Sci. 275 (1975) 225–251.
[31] H.E. Malde, The Yahoo Clay, a lacustrine unit impounded by the McKinney Basalt in the Snake River Canyon near Bliss, Idaho, Idaho Bureau of Mines and Geology, 1982.
[32] H.T. Stearns, L. Crandall, W.G. Steward, Geology and groundwater resources of the Snake River Plain in southeastern, Idaho (1938). 268 pp.
[33] H.E. Malde, The catastrophic late Pleistocene Bonneville Flood in the Snake River Plain, vol. 596, Idaho, US Geological Society Professional Paper, 1968, p. 52.
[34] J.E. O'Connor, Hydrology, Hydraulics, and Geomorphology of the Bonneville Flood, Boulder, CO, 1993. 83 pp.
[35] V.R. Baker, The channels of Mars, University of Texas Press, 1982. 198 pp.
[36] J.F. Ziegler, Helium: stopping powers and ranges in all elemental matter, Pergamon Press, New York, 1977. 367 pp.
[37] M.D. Kurz, J.J. Gurney, W.J. Jenkins, D.E. Lott, Helium isotopic variability within single diamonds from the Orapa Kimberlite Pipe, Earth Planet. Sci. Lett. 86 (1987) 57–68.
[38] D.W. Graham, L.M. Larsen, B.B. Hanan, M. Storey, A.K. Pedersen, J.E. Lupton, Helium isotope composition of the early Iceland mantle plume inferred from the tertiary picrites of West Greenland, Earth Planet. Sci. Lett. 160 (1998) 241–255.
[39] D.R. Hilton, K. Gronvold, C.G. Macpherson, P.R. Castillo, Extreme He-3/He-4 ratios in northwest Iceland: constraining the common component in mantle plumes, Earth Planet. Sci. Lett. 173 (1999) 53–60.
[40] M. Moreira, P. Madureira, Cosmogenic helium and neon in 11 Myr old ultramafic xenoliths: consequences for mantle signatures in old samples, Geochem. Geophys. Geosyst. 6 (2005).
[41] X.Z. Luo, M. Rehkamper, D.C. Lee, A.N. Halliday, High precision Th-230/Th-232 and U-234/U-238 measurements using energy-filtered ICP magnetic sector multiple collector mass spectrometry, Int. J. Mass Spectrom. 171 (1997) 105–117.
[42] K.H. Rubin, Analysis of Th-232/Th-230 in volcanic rocks: a comparison of thermal ionization mass spectrometry and other methodologies, Chem. Geol. 175 (2001) 723–750.
[43] S. Richter, S.A. Goldberg, Improved techniques for high accuracy isotope ratio measurements of nuclear materials using thermal ionization mass spectrometry, Int. J. Mass Spectrom. 229 (2003) 181–197.
[44] C.J. Allegre, M. Condomines, Fine chronology of volcanic processes using 238U–230Th systematics, Earth Planet. Sci. Lett. 28 (1976) 395–406.
[45] T.E. Cerling, Dating geomorphologic surfaces using cosmogenic He-3, Quat. Res. 33 (1990) 148–156.
[46] T.E. Cerling, H. Craig, Cosmogenic He-3 production-rates from 39-degrees-N to 46-degrees-N Latitude, Western USA and France, Geochim. Cosmochim. Acta 58 (1994) 249–255.

Please cite this article as: S.M. Aciego et al., Combining [^{3}He] cosmogenic dating with U–Th/He eruption ages using olivine in basalt, Earth Planet. Sci. Lett. (2007), doi:10.1016/j.epsl.2006.11.039

[47] J.M. Licciardi, M.D. Kurz, P.U. Clark, E.J. Brook, Calibration of cosmogenic He-3 production rates from Holocene lava flows in Oregon, USA, and effects of the Earth's magnetic field, Earth Planet. Sci. Lett. 172 (1999) 261–271.
[48] T.J. Dunai, J.R. Wijbrans, Long-term cosmogenic He-3 production rates (152 ka–1.35 Ma) from Ar-40/Ar-39 dated basalt flows at 29 degrees N latitude, Earth Planet. Sci. Lett. 176 (2000) 147–156.
[49] T.J. Dunai, Influence of secular variation of the geomagnetic field on production rates of in situ produced cosmogenic nuclides, Earth Planet. Sci. Lett. 193 (2001) 197–212.
[50] J. Dunne, D. Elmore, P. Muzikar, Scaling factors for the rates of production of cosmogenic nuclides for geometric shielding and attenuation at depth on sloped surfaces, Geomorphology 27 (1999) 3–11.
[51] M.T. Heizler, F.V. Perry, B.M. Crowe, L. Peters, R. Appelt, The age of Lathrop Wells volcanic center: an Ar-40/Ar-39 dating investigation, J. Geophys. Res. Solid Earth 104 (1999) 767–804.
[52] W.D. Sharp, P.R. Renne, The Ar-40/Ar-39 dating of core recovered by the Hawaii Scientific Drilling Project (phase 2), Hilo, Hawaii, Geochem. Geophys. Geosyst. 6 (2005).
[53] O.E. Meinzer, Large springs of the United States, in: USGS (Ed.), Water Supply Paper, vol. #557, 1927, p. 93.
[54] J. O'Connor, V. Baker, Magnitudes and implications of peak discharges from glacial Lake Missoula, Geol. Soc. Amer. Bull. 104 (1992) 267–279.

Please cite this article as: S.M. Aciego et al., Combining [^{3}He] cosmogenic dating with U–Th/He eruption ages using olivine in basalt, Earth Planet. Sci. Lett. (2007), doi:10.1016/j.epsl.2006.11.039